Proton-Regulated Electron Transfers from Tyrosine to Tryptophan in Proteins: Through-Bond Mechanism versus Long-Range Hopping Mechanism

Xiaohua Chen, Laibin Zhang, Liang Zhang, Jun Wang, Haiying Liu, and Yuxiang Bu*

Center for Modeling & Simulation Chemistry, Institute of Theoretical Chemistry, Shandong University, Jinan 250100, P. R. China

Received: August 11, 2009; Revised Manuscript Received: October 26, 2009

Charge transfer between tyrosine and tryptophan residues in proteins is continuously a hot topic because of its important biological implication. On the basis of DFT calculations and ab initio molecular dynamics simulations, several possible proton/electron cooperative transfer mechanisms from tyrosine to a tryptophan radical (or cation) without or with the assistence of a base in proteins are proposed in this work which range from direct proton-coupled π-electron π-channel/σ-channel transfers ($PC^{\pi}E^{\pi}T$ versus $PC^{\pi}E^{\sigma}T$) to proton-coupled long-range hopping mechanisms depending on the peptide conformations. In general, because of a smaller ionization potential, tryptophan readily behaves as two oxidized states: dehydrogenated neutral radical and ionized radical cation. For the neutral radical, the proton/electron transfers between a tyrosine and a tryptophan radical prefer a cooperative direct coupling mode through the $PC^{\pi}E^{\pi}T$ or $PC^{\pi}E^{\sigma}T$ mechanism if two residues are proximal or can approach each other, while they cannot take place without assistence if two residues are far apart. The tryptophan radical cation prefers to form a complex with tyrosine to stabilize the hole when two residues are proximal or can approach each other. However, the electron transfer from tyrosine to tryptophan could occur via a hopping mechanism but is regulated by a base as a proton acceptor in the vicinity of tyrosine when two residues are separated. The dynamics properties and characters for these transfer events are also presented. The energetics comparison indicates that the energy barriers for the direct PCET ($PC^{\pi}E^{\pi}T$ or $PC^{\pi}E^{\sigma}T$) mechanisms are higher than those of the base-assisting hopping mechanism (6.8−12.5 versus $\leq$4.9 kcal/mol), implying the latter is a favorable way for the proton/electron cooperative transfers. Hopefully, this work provides some helpful information for understanding the mechanisms of physiologically important electron transfer reactions.

Introduction

Exploration of the intramolecular or intermolecular electron transfer between tyrosine and oxidized tryptophan residues has important physical, chemical, and biological implications.[1−3] Especially, it is of critical importance to understand the workings of several native biological systems,[4−10] such as DNA photolyase,[6] bovine serum albumin,[7] hen egg-white lysozyme,[1,5,8] *Escherichia coli* ribonucleotide reductase,[10] nitrite reductase in *Achromobacter cycloclastes*,[11] and others. For example, electron transfer from tyrosine to the tryptophyl radical was demonstrated to be an essential step in the process leading to the active form of photolyase (fully reduced form ($FADH^-$)) in *Anacystis nidulans*.[6] A mechanism was proposed in which a tyrosine at the surface of this protein releases an electron to the three-tryptophan chain (Trp390, Trp367, Trp314), and then the electron reaches to the excited $FADH^{\bullet}$, yielding $FADH^-$.[12] Besides, in the R2 subunit of *E. coli* ribonucleotide reductase, electron transfer from Trp48 to Tyr122 radical cation is the first step, and that from Tyr356 to Trp48 is the second step in this 35 Å long-range electron transport.[10a,12,13] In addition, it has also been clarified that the electron tunneling transfer from Tyr203 to Trp144 is an important step between *Achromobacter cycloclastes pseudoazurin* and *Achromobacter cycloclastes nitrite reductase*.[11b] Clearly, all these indicate that the electron transfer between tyrosine and tryptophan is involved more generally in radical enzymes and in electron transfer proteins.

Several attempts have been undertaken to explain the electron transfer mechanisms from tyrosine to the tryptophyl cation (radical), and electron hopping and bridge-assisted superexchange mechanisms have been proposed for them, as supported by experimental evidence and theoretical calculations.[14−16] The latter, bridge-assisted superexchange, may be further subdivided into through-space, through-bond, and through-nonbonded interactions according to the varying distances and the properties of the bridges between tyrosine and tryptophan residues.[15,17,18] However, it should be emphasized that the electron transfer between tyrosine and tryptophan residues in proteins is governed by the ambient acid−base conditions.

It is well-known that the hydroxyl group of tyrosine or the imino group of tryptophan are inclined to lose their protons when the residues release or convey an electron to others in proteins, which involves a proton-coupled electron transfer (PCET) process.[19−21] As demonstrated, these proton/electron transfer processes are acid−base-catalyzed and facilitated by the favorable conformations of the peptide or protein backbone.[22] In some special conditions, aromatic rings of side chains of tyrosine and tryptophan residues are close to each other, and the proton transfer could take place directly between them. However, in most cases, these two residues are far away from each other in proteins, and there are other proton acceptors near the aromatic rings, such as lysine, histidine, and aspartic acid,[23] which play an important role in controlling the protonation state of the tyrosine and tryptophan residues and regulate directionality of the electron transfer in proteins.[10b] Therefore, electron transfer

* Corresponding author. E-mail: byx@sdu.edu.cn.

10.1021/jp9077689
Published on Web 11/19/2009

SCHEME 1: Proton-Regulated Long-Range Electron-Hopping Mechanism

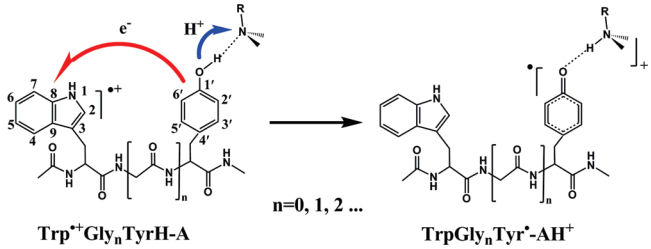

between these two residues is complicated and occurs more possibly via various PCET mechanisms subject to protein environments and conformational changes.

A lot of enzymes employ PCET reactions to fulfill efficiently charge transfer and energy transport because PCET reactions require minimal cost. These PCET reactions in the biological processes are mainly divided into two categories: collinear PCET and differently directed PCET.[12c] In the collinear PCET reactions, the electron and proton are synchronously conveyed in the same direction with different pathways,[24−28] which are prevalent in photosynthesis, respiration, lipoxygenase,[29] galactose oxidase,[30] and others. In the latter case, the electron transfer and proton transfer pathways are not in parallel, which are differently directed.[31] In this case, the distance of proton migration is short, but the electron may transfer or hop over a long distance, which is of some significance in understanding long-range electron transfer or enzyme reactions in proteins.[10,32−35] Therefore, understanding of the different forms of PCET is of crucial importance in unraveling the workings of biological systems. In this work, the major aim is to explore the possible PCET dynamics mechanisms between tyrosine and tryptophan residues in proteins.

Though a lot of works have been devoted to investigating the electron transfer between tyrosine and tryptophan residues in simple peptides and proteins, the visual images of electron transfer mechanisms between them are still not known up to now. Also, the role of the side chain of lysine or histidine in regulating the long-range electron transfer between these active sites has been unexplored as of yet. Thus, to better understand the mechanisms of electron transfer between tyrosine and tryptophan residues in proteins and elucidate possible biological implications of PCET reactions, a series of bridged donor−acceptor complexes, Trp•Gly$_n$Tyr and Trp•⁺Gly$_n$Tyr···A (n = 0, 1, 2, ..., and A denotes methylamine to mimic the amino groups of amino acid side chains[23]), were considered by carrying out density functional theory (DFT) calculations and ab initio molecular dynamics (AIMD) simulations in the present work. Herein, we report the preliminary results of DFT calculations and AIMD simulations which provide evidence for how a proton and an electron cooperatively transfer between the tyrosine and tryptophan sites. The most essential feature of the cooperative transfer mechanism of a proton and an electron is either a direct PCET mechanism or a proton-regulated long-range electron hopping transfer (PCEH) mechanism (see Scheme 1) between the active sites of the residues, depending on the separation and protonation state or hydrogen-bonding modes of the two sites. Hopefully, this study will provide an unambiguous concept and dynamic picture for understanding proton-driven electron-transfer reactions from tyrosine to tryptophan residue in proteins.

General Considerations and Details of Calculations and Simulations

To systematically explore all possible mechanisms for the electron transfer between the aromatic rings of tyrosine and tryptophan residues in proteins, different situations were considered. Since tryptophan is a more hole-preferred site than tyrosine with smaller ionization potential (IP = 7.19 eV versus 7.50 eV of tyrosine), tryptophan is generally oxidized upon hole attack or photoinduced ionization. Thus, two states for the oxidized tryptophan are possible: tryptophan radical cation (Trp•⁺) and its dehydrogenated radical (Trp•). Further, different separations between two residue active sites were also considered here to examine the distance dependence of electron transfer dynamics via direct exchange or long-range hopping mechanism. Actually, when two residues are close to each other, they prefer to bind cooperatively to a hole upon hole-trapping for the sake of stabilization, forming a cation dimer complex without an unambiguous intermolecular electron transfer. Thus, such a case with direct coupling between two active sites (Tyr···Trp•⁺) was removed from this consideration. However, the oxidized tryptophan (Trp•⁺) more readily releases a proton to the proximal basic group, becoming a neutral radical (Trp•). This radical could weakly interact with its proximal Tyr phenol group, presenting a condition for possible electron/proton exchange between them. Clearly, when the separation between Trp• and a possible Tyr is large, the electron/proton exchanges between two active sites are impossible because of no direct coupling and also no deriving force for the transfer. Overall, only two cases were examined in this study which include the directly interacting Tyr···Trp• and the differently separated Tyr···Trp•⁺ assisted by a basic group of a certain residue for exploration of their possible proton/electron transfer mechanisms. In addition, as a simplified model, 4-methylphenol (Tyr) and the 3-methylindolyl (Trp) radical were employed to examine the direct proton/electron transfer exchange between Tyr and the Trp• radical in two approximal main chains. Similarly, several hydrogen bonding modes between Tyr phenol and Trp indole radical were also designed by changing the intervening Gly residues as Trp•Gly$_n$Tyr radical (n = 0, 1, 2) to realize the straightforward proton/electron transfer between them. The last case is that no direct coupling interaction between two aromatic side chains (phenol versus indole) exists, but a methylamine modeling basic groups such as a Lys amino group or His imidazole is considered to hydrogen bond to the phenol group as a proton acceptor like those in proteins,[1,4] as shown as Trp•⁺Gly$_n$TyrH···A (n = 0, 1, 2, 3, 4, 5) in Scheme 1.

All gas-phase calculations were carried out by using the Gaussian 03 suite of programs.[36] The UB3LYP[37] hybrid functional in conjunction with the 6-31+G(d,p) basis set[38] was utilized to fully optimize the geometries of relative small systems and to perform the harmonic vibrational analyses for confirming minima (all real frequencies) and transition state structures (one imaginary frequency). A large basis set, 6-311++G(d,p), was used to verify reliability of 6-31+G(d,p) upon the reactions between 4-methylphenol and 3-methylindole radical. For their geometries, B3LYP shows essentially no dependence on a change in the size and flexibility of the basis set. Additionally, an unrestricted Hartree−Fock (UHF) method with a 6-31+G(d,p) basis set was used to examine the electron transfer in Trp•⁺TyrH···A. Besides, the hybrid DFT BHandHLYP functional, based on one-half of HF exchange and one-half of the density functional theory (DFT) exchange including local (LSDA) and gradient-corrected (Becke88) terms (correlation is based on the LYP functional), was used to examine the proton/

electron transfer mechanisms of the Trp•Tyr radical and Trp•+TyrH···A (the details for the calculations are given in the Supporting Information). All these validated that it is appropriate to use the UB3LYP method with a 6-31+G(d,p) basis set to probe the electron/proton transfer reaction in Trp•Gly$_n$Tyr and Trp•+Gly$_n$TyrH···A (n = 0, 1, 2, ...). Due to the large computational cost, only the UB3LYP/6-31G(d)[39] method was carried out for the geometries of relatively big systems, Trp•+Gly$_n$TyrH···A (n = 1−4). To obtain more accurate reaction energies, single-point energies were recalculated for all the reactants, transition states, and products at the B3LYP/6-31+G(d,p)//B3LYP/6-31G(d) level of theory. Moreover, the intrinsic reaction coordinate (IRC)[40] analyses were made at the corresponding levels of theory for all complexes to ensure the connections of the transition states with the desired reactants and products. The restricted molecular orbital contours were used to display the orbital character.

To validate the base-catalyzed proton-coupled long-range electron-hopping processes from tyrosine to the tryptophan radical cation in different distances with a methylamine hydrogen bonding to phenol as a proton acceptor, ab initio molecular dynamics (AIMD) simulations were performed with the DMol[341] upon the structures obtained by the B3LYP/6-31+G(d,p) and B3LYP/6-31G(d) optimizations, as implemented in the Accelrys' Cerius2 package.[42] The DMol^3 calculations were done at the DFT level with the generalized gradient approximation (GGA) corrected-exchange potential of the BLYP (the Lee−Yang−Parr correlation functional).[37,43] We chose a basis set composed of a double numerical atomic orbital augmented by a polarized function for heaven atoms (DND), and all-electron symmetry-unrestricted calculations were performed. The energy tolerance in the self-consistent field calculations was set to 1.0×10^{-5} eV. The simulations on all polypeptide models were carried out in a canonical *NVT* ensemble and total simulation time of 6.0 ps with a time step of 1.0 fs. Temperature was kept constant (300 K) by using Massive GGM.[44] In addition, it should be noted that the energies instead of enthalpies are used in the relevant analyses.

Results and Discussions

Proton/Electron Transfers between Tyr and Trp• in Approximal Peptide Chains. The case of close proximity of tyrosine and tryptophan residues lying in two different main chains occurs frequently in some structures of proteins. For example, Tyr65 and Trp128 in phycobilisomes are close and play roles in energy transfer and electron transfer from phycoviolobilin to the photosynthetic reaction centers within the thylakoid membrane (Figure S17, Supporting Information).[45] 4-Methylphenol (Tyr) and 3-methylindole (Trp) are selected to model tyrosine and tryptophan for examining the possibility of electron transfer between these two residues in different main chains with proximal aromatic rings. The optimized structures of reactant (Tyr−Trp•), transition state (Tyr−Trp•^{ts}), and product (Tyr•−Trp) with the main parameters are displayed in Figure 1. It is clear that the two moieties of complexes are linked by an intermolecular hydrogen bond, the N···H length of 1.85 Å for Tyr−Trp• and the O···H length of 1.97 Å for Tyr•−Trp. The planes of phenol and indole in these two complexes are nearly orthogonal. The binding energies for Tyr−Trp• and Tyr•−Trp are 9.2 and 6.4 kcal/mol, respectively. When going to transition state, Tyr−Trp•^{ts}, two aromatic rings are nearly coplanar. Tyr−Trp•^{ts} lies 6.8 kcal/mol in energy above Tyr−Trp• and 10.0 kcal/mol above Tyr•−Trp, which indicates that the proton/electron transfers from Tyr to Trp• are more favorable than its inverse process.

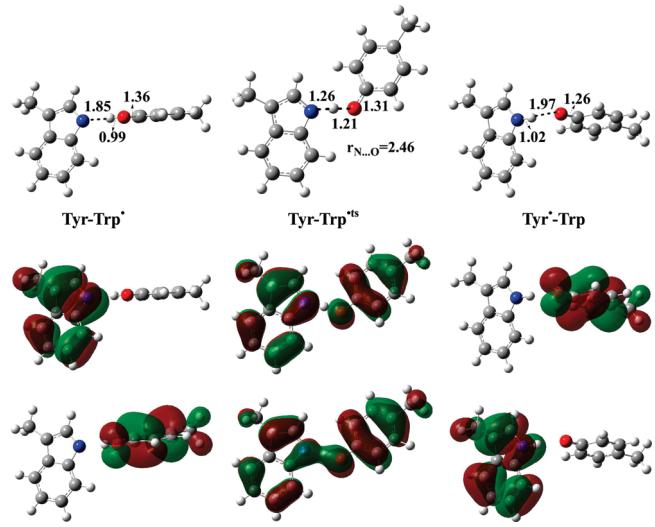

Figure 1. Geometries of the 4-methylphenol and 3-methylindole radical couple from reactant, transition state, to product with main parameters and the corresponding singly occupied molecular orbitals (SOMOs) and highest doubly occupied molecular orbitals (HDMOs).

Mulliken molecular orbital analyses reveal that the singly occupied molecular orbital (SOMO) mainly localizes over the aromatic rings of the indolyl radical for Tyr−Trp• and over the aromatic ring and O-atom of the phenoxyl radical for Tyr•−Trp with π-orbital characters, as shown in Figure 1. Besides, the highest doubly occupied molecular orbital (HDMO) mainly localizes over the other aromatic ring in respect to SOMO with π-orbital character for both complexes. However, for Tyr−Trp•^{ts}, SOMO and HDMO delocalize over the whole framework of the complex. The former is a π-antibonding and the latter a π-bonding, and their combination forms a three-electron π-bond, a clear π-channel for electron transfer. These observations suggest that the proton/electron transfer reactions from phenol to indolyl radical proceed via a typical proton-coupled π-electron π-channel transfer (PC$^\pi$E$^\pi$T) mechanism[46] with a proton migration from the O-atom lone pair to the N-atom lone pair in the plane of the complex and at the same time an electron transfer from a doubly occupied π-orbital localized on the phenol moiety to the singly occupied π-orbital on the indole moiety in the same direction. This mechanism is similar to that in the phenol/phenoxyl couple (also PC$^\pi$E$^\pi$T)[24] but with a slight difference in which a considerable conformation rotation is required in going to the transition state for the former to produce a favorable π-channel to electron transfer. Clearly, this asymmetric PCET reaction is conformation controlled.

Proton/Electron Transfers between Tyr and Trp• in the Same Peptide Chain. In some cases, both tyrosine and tryptophan residues reside in the same peptide chain in which two residues are separated by some other intervened amino acid residues in proteins. Clearly, conformations of Tyr···Trp• in the same peptide chain different from those in different peptide chains mentioned above implies different proton/electron transfer mechanisms. In the past years, the intramolecular one-electron transfer reactions from tyrosine to the tryptophan radical have been extensively investigated,[2,4,17,22,47,48] and two mechanisms were proposed in which an electron transfers via a superexchange mechanism for the short distance or via a sequential hopping mechanism for the long distance. Furthermore, the electron transfer is generally coupled with proton transfer(s). In particular, on the basis of experimental rate constants of electron transfer, Jovanovic et al. suggested a stepwise mechanism, proton transfer followed by electron transfer, for proton/

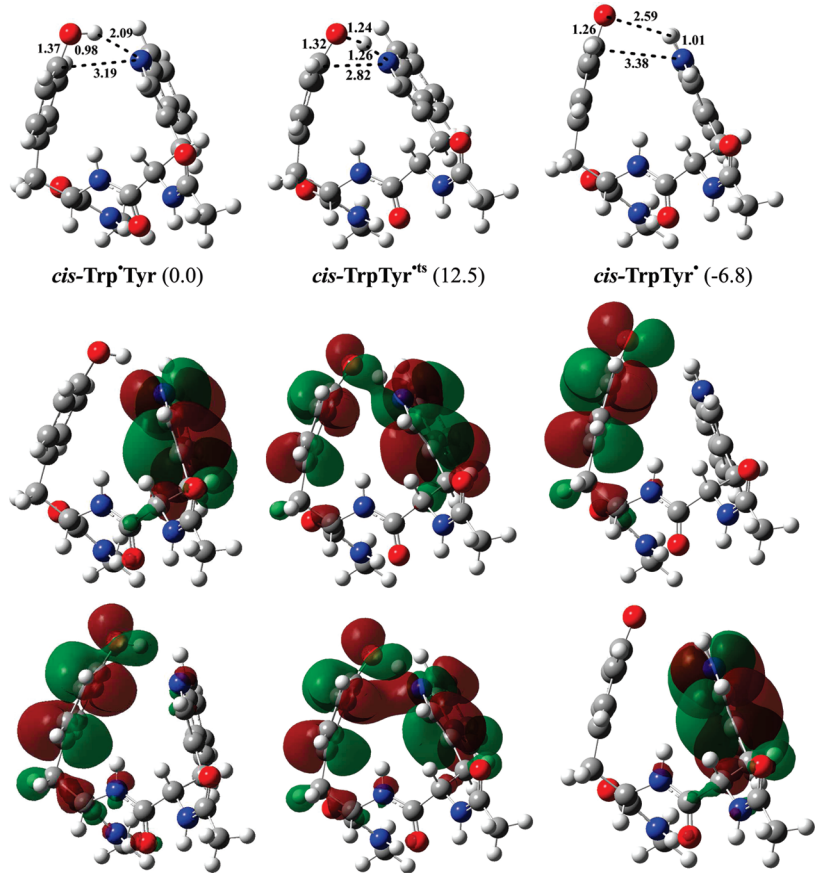

Figure 2. Geometries of *cis*-TrpTyr radical from reactant, transition state, to product with main parameters and the corresponding singly occupied molecular orbitals (SOMOs) and highest doubly occupied molecular orbitals (HDMOs).

electron transfers in a Tyr−Trp• dipeptide radical,[22] while Faraggi et al. reported that the rate constant of electron transfer is not sensitive to the distance between aromatic amino acid residues in the small peptide Tyr-$(Pro)_n$-Trp ($n = 0-3$) radicals.[2] Undoubtedly, due to constraint of the peptide backbone, two reactive aromatic rings cannot interact via a favorable coupling mode (Figure 1) for the proton/electron transfer. Thus, different mechanisms from that in Figure 1 are expected for their possible proton/electron transfers.

As envisioned, our DFT calculations indicate that the intramolecular electron transfer reactions between tyrosine and the tryptophan radical in the oligopeptides could change subject to the different conformations and surrounding environment. When the aromatic rings of tyrosine and tryptophan residues lie in the same side of the main chain and are linked by an intramolecular hydrogen bond, the proton/electron transfer reactions between them occur via a typical PCET mechanism.

The structures of the reactant, transition state, and the product for the *cis*-TrpTyr radical with main parameters are shown in Figure 2. For the reactant, *cis*-Trp•Tyr, the aromatic rings of their side chains form a face-to-face structure linked by an intramolecular hydrogen bond (the N···H length of 2.09 Å), and the $N_1-C_{1'}$ distance is 3.19 Å. In this case, SOMO mainly delocalizes over the indole ring and HDMO over the O-conjugated benzene ring in phenol. When going to the transition state, *cis*-TrpTyr•ts, the distance between the face-to-face aromatic rings becomes shorter than *cis*-Trp•Tyr, and the $N_1-C_{1'}$ distance is only 2.82 Å, which indicates a large overlap between the π-orbitals of the aromatic rings. Both SOMO and HDMO distribute over the two aromatic side chains with a partial σ-antibonding feature for the former and a σ-bonding feature for the two aromatic rings. The linear combination of these two σ-orbitals yields a three-electron σ-bond between the approximal aromatic rings, which acts as an electron transfer channel between tyrosine and tryptophan (Figure 2). For the product, *cis*-TrpTyr•, the transferring proton is bonded to the N-atom of the indole moiety, and the SOMO completely delocalizes over the O-conjugated benzene ring in the phenol moiety. Therefore, it can be safely concluded that the proton/electron exchange in the *cis*-Trp•Tyr radical takes place via a proton-coupled π-electron σ-channel transfer ($PC^{\pi}E^{\sigma}T$) mechanism with a proton migration between O and N atoms and an electron transfer through a three-electron σ-bond formed by the $\pi-\pi$ interaction of two aromatic rings. This mechanism is similar to another mode for the formal H-atom exchange between the tyrosine and tyrosyl in ribonucleotide reductases with a σ-channel[25b] instead of a π-channel[24,25a] electron transfer.

A similar mechanism can be found for the intramolecular proton/electron transfers in the *cis*-TrpGlyTyr radical system: a $PC^{\pi}E^{\sigma}T$ mechanism (see Figure S1, Supporting Information). However, for the *cis*-$TrpGly_2Tyr$ radical system (Figure S2, Supporting Information), the electron/proton transfer reactions proceed via a $PC^{\pi}E^{\pi}T$ mechanism similar to that in Tyr···Trp• but with a slight bending indole−phenol coplane due to the constraint of the peptide backbone. Clearly, this should be attributed to the fact that large separation does not favor the direct face-to-face $\pi-\pi$ coupling interaction between two aromatic rings and, instead, does favor the $\pi-\pi$ superconjugating interaction in the *cis*-$TrpGly_2Tyr$ radical. From this observation, we could rationally predict that for other *cis*-Trp•$(Gly)_n$Tyr radicals with large separation ($n > 2$) between two active centers the formal H-atom exchange occurs via the

TABLE 1: Corresponding Forward [E_a(f)] and Backward [E_a(b)] Energy Barriers of the Direct PCET Reactions between the Aromatic Rings of Tyrosine and the Tryptophan Radical

	Trp$^{\bullet}$−Tyr	*cis*-Trp$^{\bullet}$Tyr	*cis*-Trp$^{\bullet}$GlyTyr	*cis*-Trp$^{\bullet}$Gly$_2$Tyr
E_a(f) (kcal/mol)	6.8	12.5	10.5	9.6
E_a(b) (kcal/mol)	10.0	19.2	11.4	6.7

PC$^{\pi}$E$^{\pi}$T mechanism. Actually, this coplanar arrangement is both energetically and structurally favorable to the proton/electron transfers between them because of the rigidity reduction of the peptide backbone. Data in Table 1 have clearly justified our analyses. That is, the energy barriers for the intramolecular proton/electron transfer reactions in the *cis*-Trp$^{\bullet}$Gly$_n$Tyr systems (n = 0, 1, 2) decrease with the increase of the intervening glycine residues, indicating that a PC$^{\pi}$E$^{\pi}$T mechanism is generally more preferred than a PC$^{\sigma}$E$^{\pi}$T one for the electron/proton transfers in this kind of system.

Base-Assisting Proton/Electron Long-Range Transfers. Clearly, the mechanisms mentioned above require a direct coupling contact between the donor and acceptor centers which provide molecular orbital overlap as the electron transfer channel and hydrogen bonding as a proton transfer pathway. For the Trp$^{\bullet}$-(peptide)$_n$-Tyr systems with more intervening peptide units, although the flexible peptide chains can bend more possibly to meet the requirement for a favorable structure to the proton/electron transfers, the relatively rigid polypeptide helices and protein structures can undoubtedly constrain their flexibility, leading to noncontacted arrangements of two active sites. Thus, the proton/electron transfers between them are impossible in this case if no other assisting groups coexist with them. However, nature provides plentiful diversity for the most optimized functions of proteins. In many proteins, basic groups, such as the side chains of lysine or histidine, are generally available around these active sites with hydrogen bonds to them (see Figures S18 and S19 and their references therein for natural proteins, Supporting Information). Thus, the proton and electron may alternatively choose other ways to realize their transfers between two active sites under the assistance of a basic group. In this section, we report a proton-regulated electron hopping mechanism and give a dynamic picture how the proton/electron cooperatively transfer in terms of DFT calculations and AIMD simulations.

When the side-chain groups (indole and phenol) of tyrosine and tryptophan residues are far away from each other (the shortest distance ($r_{H5-C4'}$) between indole and phenol moieties is 6.55 Å in the Trp$^{\bullet+}$TyrH radical cation, where TyrH also denotes tyrosine with an emphasis on its hydroxyl H because it is released to a base in a base-assisting mechanism), the spin density mainly resides in the aromatic rings of tryptophan and an approximal O-atom of the peptide backbone unit, as shown in Figure 3, because of a lower redox potential of the indole moiety than that of the phenol moiety. In the structure of Trp$^{\bullet+}$TyrH, the distance between the approximal O-atom and C_2 of the indole moiety is only 2.64 Å, and this electron-rich O-atom plays an important role in stabilizing the electron-deficient aromatic rings of the tryptophan cation.[49] When a base modeled by a methylamine approaches to the phenol moiety of Trp$^{\bullet+}$TyrH, it may serve as a proton acceptor and plays an important role in promoting an intramolecular electron transfer from the phenol moiety to the indolyl cation moiety. In the reactant complex Trp$^{\bullet+}$TyrH···A, where A denotes a methylamine, an intermolecular hydrogen bond is formed between the phenol moiety and methylamine, as shown in Figure 4, with a

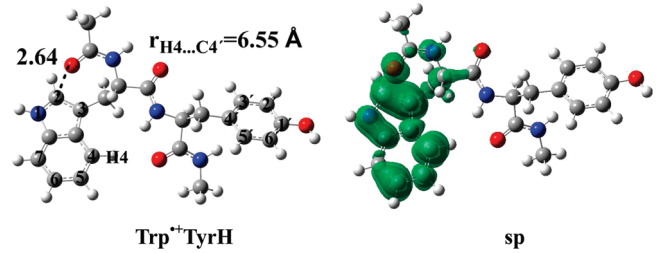

Figure 3. Geometry of the Trp$^{\bullet+}$TyrH radical cation with main parameters and the corresponding spin density surface (sp).

H···N distance of 1.70 Å. Besides, a carboxyl O of peptide framework points to the pyrrole ring of the indole group with a short distance of 2.76 Å between the O and C_2 of indole, indicating a strong interaction between them.[49] The Mulliken spin density analysis reveals that the unpaired electron resides mainly on the tryptophan moiety (83%) and partly on the phenol moiety (17%), implying that a part of the electron transfers from tyrosine to tryptophan when methylamine presents near the side chain of the tyrosine residue with respect to Trp$^{\bullet+}$TyrH. At its transition state (Trp$^{\bullet}$TyrH^{+}···A^{ts}), the migration proton lies nearly in the middle between the N of methylamine and the O of the phenol group. In this case, the unpaired electron resides on both the phenol (59%) and the indole group (40%). The energy barrier for the proton/electron transfers in this system is predicted to be only 4.7 kcal/mol. For its product, TrpTyr$^{\bullet}$···H^{+}A, the migrating proton is bonded to the N of methylamine (1.11 Å for the H−N bond length). TrpTyr$^{\bullet}$···H^{+}A is only 1.5 kcal/mol above Trp$^{\bullet+}$TyrH···A in energy. Two factors are recognized in stabilizing TrpTyr$^{\bullet}$···H^{+}A to be a strong intermolecular hydrogen bond formed between the phenoxy O and methylaminium H^{+}, and a special intramolecular H$^{\delta+}$···π interaction yielded between a peptide backbone unit H$^{\delta+}$ and the aromatic rings of indole group, as shown in Figure 4. In the latter, the shortest distance between the H and the aromatic rings (C_9) is 2.75 Å, implying that this H$^{\delta+}$···π is considerably strong. The Mulliken spin density analysis reveals that the unpaired electron localizes entirely over the tyrosine group in TrpTyr$^{\bullet}$···H^{+}A, indicating that an electron transfers from the phenol to the indole with respect to Trp$^{\bullet+}$TyrH···A. Besides, during this reaction process, the shortest distance between the indole and phenol groups is 5.64 Å, which indicates that the direct molecular orbital overlap between the two far-separated aromatic side chains is impossible. Therefore, we infer that an electron hops from the tyrosine to the tryptophan group during this process, and at the same time a proton migrates from an O-centered lone pair orbital of the phenoxy moiety to a N-centered lone pair orbital of methylamine at a different direction. In this process, since the proton transfer is the rate-determining step and governs the electron hopping, the overall mechanism with respect to this cooperative proton/electron transfer process could be described as a proton-regulated electron hopping transfer one (PCEH, Scheme 1).

Dynamics Character of the PCEH Mechanism. To gain further insight into the dynamic behavior of proton/electron in the Trp$^{\bullet+}$TyrH···A system in their cooperative transfer process, Trp$^{\bullet+}$TyrH···A was put in a periodically repeated cubic cell (30.0 × 21.0 × 21.0 Å^3) by carrying out ab initio molecular dynamics (AIMD) simulations for a 6.0 ps simulation period. In the period of the first 1.0 ps, Trp$^{\bullet+}$TyrH and methylamine (A) are linked by an intermolecular O−H···N hydrogen bond between the phenol OH and the methylamine N, and the unpaired electron mainly resides on the indole group. Afterward, the O···H distance starts to lengthen and the N···H distance

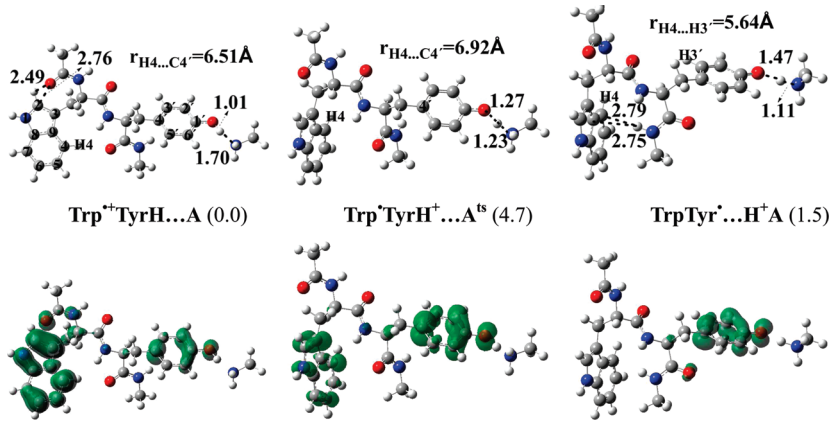

Figure 4. Geometries of the Trp•+TyrH···A radical cation from reactant, transition state, to product with main parameters and the corresponding total spin density surfaces. The numbers in the parentheses are the relative energies with respect to reactant.

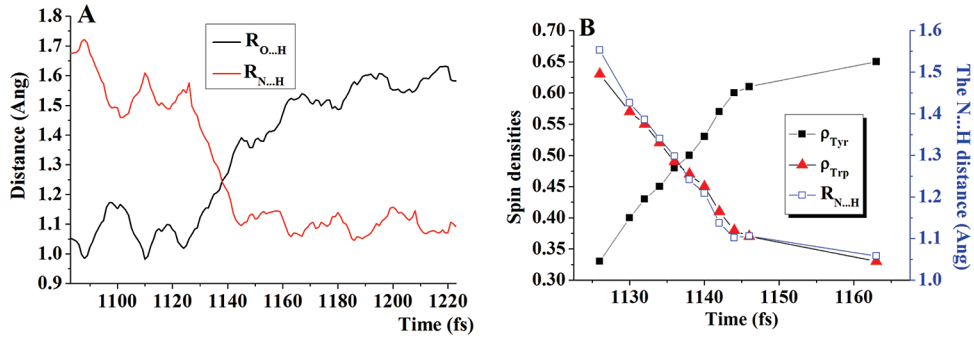

Figure 5. (A) Proton migration process for the simulation of the Trp•+TyrH···A radical cation which is described by the changes of O···H and N···H distances, indicating that the O−H is broken and the N−H is formed in the time range of 1083−1192 fs. (B) The spin densities on tyrosine moiety (ρ_{Tyr}) and tryptophan moiety (ρ_{Trp}) change along the dynamics trajectory with the varying N···H distance.

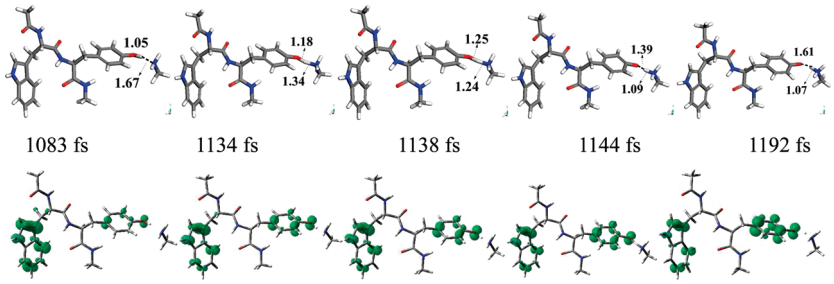

Figure 6. Several snapshots of representative structures (up) with main parameters of ab initio MD simulations of the Trp•+TyrH···A radical cation and the corresponding total spin density surfaces (down), shown along the dynamics trajectory. The number under the picture is the simulation time.

to shorten at the same time, indicating a proton transfer from the phenol O to the methylamine N. The proton/electron migration dynamics trajectory and relevant changes with respect to the evolution time for Trp•+TyrH···A are displayed in Figure 5. Besides, some representative structures with main parameters in this process and the corresponding spin density surfaces are reported in Figure 6. Figure 5(A) clearly indicates that the proton migration is very fast in the time range of 1125−1145 fs. At 1083 fs, the transferring proton is bonded to the phenoxy O, and two separated parts of the complex are linked by an intermolecular hydrogen bond (1.67 Å). In this case, the unpaired electron largely localizes on the indole moiety (71%) and only a little on the phenol moiety (22%). In contrast to the structure at 1083 fs, the O−H bond elongates to 1.18 Å, and the N···H distance shortens to 1.34 Å at 1134 fs. Distributions of the unpaired single electron on the indole and phenol moieties are 55% and 42%, respectively. As the simulation progresses, the migrating proton nearly reaches to the middle between the phenoxy O and the methylamine N at 1138 fs, and the amounts of unpaired single electron distributed on the indole (53%) and phenol (46%) moieties are nearly equal, in agreement with the aforementioned transition state obtained by DFT calculations. After 6 fs, the O···H distance lengthens to 1.39 Å, and the N···H distance becomes 1.09 Å.[50] Here, this evidence clearly indicates that the initial O−H bond in the phenol group has been broken, and a N−H bond has been formed in conjunction with an electron hopping from the phenol to the indole in the Trp•+TyrH···A system along the time evolvement. Therefore, the proton/electron transfer reactions of the Trp•+TyrH···A system may be described by a coupled way of the proton moving and electron hopping, as evidenced by the corresponding gradual changes in the O···H distance (increase), the N···H distance (decrease), and the spin density distributions on the indole moiety (decrease) and the phenol moiety (increase) during the simulation process. This AIMD simulation further substantiates the proton/electron transfer reactions in the Trp•+TyrH···A system to occur via a proton-regulated long-range electron hopping mechanism.

Besides, the $Trp^{\bullet+}Gly_nTyrH\cdots A$ systems with n intervening peptide backbone units ($n = 1-5$) have also been examined by AIMD simulations in different periodically repeated cubic cells depending on their different sizes (the details are given in the Supporting Information). The simulation results reveal that the proton/electron transfer reactions for them all occur via a proton-regulated long-range electron hopping mechanism similar to that in $Trp^{\bullet+}TyrH\cdots A$. The coupled transfer process between a proton migrating and an electron hopping are all finished within 25 fs. However, the distance of the electron donor and the acceptor increases from 8.07 Å in $Trp^{\bullet+}GlyTyrH\cdots A$ to 17.14 Å in $Trp^{\bullet+}Gly_5TyrH\cdots A$ for all considered systems. This observation implies that the rate of the electron transfer from tyrosine to the tryptophyl radical cation in the oligopeptides is nonsensitive to the distance between the electron donor and the acceptor when a methylamine presents near the tyrosine residue as a proton acceptor, in agreement with the experimental observation in a series of similar oligopeptide systems. This proton-regulated long-range electron hopping mechanism may be of some biological significance and can help us to understand the effective long-range electron transfer from the tyrosine residue to the tryptophan residue in proteins. For example, in the *E. coli* ribonucleotide reductase (RNR), the long-range electron transfer from Tyr365 to Trp48 is always elusive,[20] and the proton-coupled electron hopping mechanism could elucidate this long-range electron transfer phenomenon.[51] An electron of the side chain of Tyr365 moves to Trp48, and at the same time the hydroxyl group of Tyr365 releases a proton to the surroundings. This mechanism also indirectly supports the suggestion of Seyedsayamdost et al. that a hydrogen-bonding pathway between Trp48 and Tyr365 in RNR does not play a crucial role in assisting this long-range electron transport.[51]

Conclusions

In the present work, our investigations present possible proton/electron transfer mechanisms from the tyrosine residue to the tryptophan radical (or cation) without or with assistance of methylamine in proteins. When the side chains of these two amino acids are proximal, it is possible for a direct contact between the two aromatic rings. In this case, two aromatic rings could form a stable complex to stabilize the hole if the tryptophan moiety is an oxidized radical cation, while the proton/electron transfer reactions between tyrosine and the tryptophan radical could take place via a typical PCET mechanism if tryptophan is a dehydrogenated radical (oxidized followed by deprotonation). In the latter, if the tyrosine and the tryptophan radical are in different peptide chains, two aromatic rings may get the most optimal contact without structural constraint in the reaction process, and the proton/electron transfers could occur with a nearly coplanar transition state via a $PC^{\pi}E^{\pi}T$ mechanism with an electron of a doubly occupied π-orbital of phenol moving to the singly occupied π-orbital of the indole radical. Alternatively, if tyrosine and the tryptophan radical are in the same peptide chains and their distance is short, such as $Trp^{\bullet}Gly_nTyr$ ($n = 0, 1$), the aromatic rings of tyrosine and tryptophan are roughly parallel and the reactions proceed via a $PC^{\pi}E^{\sigma}T$ mechanism with an electron σ-channel transfer through a face-to-face overlap between the π-orbital of indole and the π-orbital of phenol. Differently, for the case of $Trp^{\bullet}Gly_2Tyr$ and even other long-separated cases, two aromatic rings could adopt a more favorable nearly coplanar geometry (if its peptide backbone is not constrained), and thus, the reactions can take place via a $PC^{\pi}E^{\pi}T$ mechanism.

When the side chains of the tryptophan and tyrosine residues are separated by the intervening $(Gly)_n$ ($n = 0, 1, 2, ...$) peptide chains and a basic group also presents near the phenol group as a proton acceptor, the reactions could occur via a proton-regulated electron hopping mechanism. That is, for the $Trp^{\bullet+}TyrH\cdots A$ system without an intervening group between two residues, the shortest distance between the indole and phenol moieties is also 5.70 Å, but an electron of phenol may hop to the indole cation in conjunction with a proton cooperative migration from the phenol O to the methylamine N. Further AIMD simulations for a series of $Trp^{\bullet+}Gly_nTyrH-A$ ($n = 0\sim5$) have verified this proton-regulated long-range electron hopping mechanism with a clear dynamic picture.

The energetics comparison indicates that the energy barriers for the direct PCET ($PC^{\pi}E^{\pi}T$ or $PC^{\pi}E^{\sigma}T$) mechanisms are higher than those of the base-assisting hopping mechanism (6.8−12.5 versus ≤4.9 kcal/mol), implying the latter is a favorable way for the proton/electron cooperative transfers. This observation has also confirmed that the electron transfer between tyrosine and tryptophan residues in proteins depends on not only the conformation but also the surrounding environment.

These results provide insight into the fundamental mechanism of electron transfer between tyrosine and tryptophan residues in proteins and also exhibit implications for a wide range of biologically important processes, where tyrosine and tryptophan residues act as electron relay stations to facilitate electron transfer. Thus, these types of calculations and simulations on the modeling systems can play an important role in understanding the concept of PCET and elucidating the mechanisms of physiologically important electron transfer reactions in proteins.

Acknowledgment. This work was supported by NSFC (20633060, 20573063), NCET, and High-performance Comput & Simulation Platform at SDU Chem School.

Supporting Information Available: The molecular geometries, molecular orbitals, distribution of spin densities, and ab initio molecular dynamics simulation results of all polypeptide radicals (cations). This material is available free of charge via the Internet at http://pubs.acs.org.

References and Notes

(1) Butler, J.; Land, E. J.; Prütz, W. A.; Swallow, A. J. *Biochim. Biophys. Acta* **1982**, *705*, 150–162.
(2) Faraggi, M.; DeFilippis, M. R.; Klapper, M. H. *J. Am. Chem. Soc.* **1989**, *111*, 5141–5145.
(3) Lee, C.-Y. *FEBS Lett.* **1992**, *299*, 119–123.
(4) Chen, Z.-W.; Koh, M.; Van Driessche, G. V.; Beeumen, J. J. V.; Bartsch, R. G.; Meyer, T. E.; Cusanovich, M. A.; Mathews, F. S. *Science* **1994**, *266*, 430–432.
(5) Weinstein, M.; Alfassi, Z. B.; DeFelippis, M. R.; Klapper, M. H.; Faraggi, M. *Biochim. Biophys. Acta* **1991**, *1076*, 173–178.
(6) Aubert, C.; Mathis, P.; Eker, A. P. M.; Brettel, K. *Proc. Natl. Acad. Sci. U.S.A.* **1999**, *96*, 5423–5427.
(7) Mukherjee, T.; Joshi, R. *Biophys. Chem.* **2003**, *103*, 89–98.
(8) Bobrowski, K.; Holcman, J.; Poznanski, J.; Wierzchowski, K. L. *Biophys. Chem.* **1997**, *63*, 153–166.
(9) Stuart-Audette, M.; Blouquit, Y.; Faraggi, M.; Sicard-Roselli, C.; Houée-Leven, C.; Jollés, P. *Eur. J. Biochem.* **2003**, *270*, 3565–3571.
(10) (a) Bollinger, J. M.; Tong, W. H.; Ravi, N.; Huynh, B. H.; Edmondson, D. E.; Stubbe, J. *J. Am. Chem. Soc.* **1994**, *116*, 8024–8032. (b) Reece, S. Y.; Stubbe, J.; Nocera, D. G. *Biochim. Biophys. Acta* **2005**, *1706*, 232–238.
(11) (a) Zumft, W. G. *Microbiol. Mol. Biol. Rev.* **1997**, *61*, 533–616. (b) Yamaguchi, K.; Shuta, K.; Suzuki, S. *Biochem. Biophys. Res. Commun.* **2005**, *336*, 210–214.
(12) (a) Sancar, A. *Chem. Rev.* **2003**, *103*, 2203–2238. (b) Aubert, C.; Brettel, K.; Mathis, P.; Eker, A. P. M.; Boussac, A. *J. Am. Chem. Soc.* **1999**, *121*, 8659–8660. (c) Reece, S. Y.; Hodgkiss, J. M.; Stubbe, J.; Nocera, D. G. *Phil. Trans. R. Soc. B* **2006**, *361*, 1351–1364.
(13) (a) Sneeden, J. L.; Loeb, L. A. *J. Biol. Chem.* **2004**, *279*, 40723–40728. (b) Baldwin, J.; Krebs, C.; Ley, B. A.; Edmondson, D. E.; Huynh, B. H.; Bollinger, J. M., Jr. *J. Am. Chem. Soc.* **2000**, *122*, 12195–12206. (c)

Bollinger, J. M.; Tong, W. H.; Ravi, N.; Huynh, B. H.; Edmonson, D. E.; Stubbe, J. *J. Am. Chem. Soc.* **1994**, *116*, 8015–8023.

(14) Long, Y.-T.; Abu-Irhayem, E.; Kraatz, H.-B. *Chem.—Eur. J.* **2005**, *11*, 5186–5194.

(15) Isied, S. S.; Ogawa, M. Y.; Wishart, J. F. *Chem. Rev.* **1992**, *92*, 381–394.

(16) (a) Petrov, E. G.; Shevchenko, Ye. V.; Teslenko, V. I.; May, V. *J. Chem. Phys.* **2001**, *115*, 7107–7122. (b) Ostapenko, M. G.; Petrov, E. G. *Phys. Status Solidi B* **1989**, *152*, 239–247.

(17) (a) DeFelippis, M. R.; Faraggi, M.; Klapper, M. H. *J. Am. Chem. Soc.* **1990**, *112*, 5640–5642. (b) Bobrowski, K.; Holcman, J.; Poznanski, J.; Ciurak, M.; Wierzchowski, K. L. *J. Phys. Chem.* **1992**, *96*, 10036–10043. (c) Mishra, A. K.; Chandrasekar, R.; Faraggi, M.; Klapper, M. H. *J. Am. Chem. Soc.* **1994**, *116*, 1414–1422.

(18) Polo, F.; Antonello, S.; Formaggio, F.; Toniolo, C.; Maran, F. *J. Am. Chem. Soc.* **2005**, *127*, 492–493.

(19) Aubert, C.; Vos, M. H.; Mathis, P.; Eker, A. P. M.; Brettel, K. *Nature* **2000**, *405*, 586–590.

(20) Stubbe, J.; Nocera, D. G.; Yee, C. S.; Chang, M. C. Y. *Chem. Rev.* **2003**, *103*, 2167–2202.

(21) (a) Shih, C.; Museth, A. K.; Abrahamsson, M.; Blanco-Rodriguez, A. M.; Di Bilio, A. J.; Sudhamsu, J.; Crane, B. R.; Ronayne, K. L.; Towrie, M.; Vlček, A.; Richards, J. H.; Winkler, J. R.; Gray, H. B. *Science* **2008**, *320*, 1760–1762. (b) Bollinger, J. M., Jr. *Science* **2008**, *320*, 1730–1731.

(22) Jovanovic, S. V.; Harriman, A.; Simic, M. G. *J. Phys. Chem.* **1986**, *90*, 1935–1939.

(23) (a) Pond, A. E.; Ledbetter, A. P.; Sono, M.; Goodin, D. B.; Dawson, J. H. *Electron Transfer in Chemistry*; Balzani, V., Ed.; Wiley-VCH: Weinheim, Germany, 2001; Vol. 3.1.4, pp 56−104. (b) Ferreira, K. N.; Iverson, T. M.; Maghlaoui, K.; Barber, J.; Iwata, S. *Science* **2004**, *303*, 1831–1838.

(24) Mayer, J. M.; Hrovat, D. A.; Thomas, J. L.; Borden, W. T. *J. Am. Chem. Soc.* **2002**, *124*, 11142–11147.

(25) (a) DiLabio, G. A.; Ingold, K. U. *J. Am. Chem. Soc.* **2005**, *127*, 6693–6699. (b) DiLabio, G. A.; Johnson, E. R. *J. Am. Chem. Soc.* **2007**, *129*, 6199–6203.

(26) Skone, J. H.; Soudackov, A. V.; Hammes-Schiffer, S. *J. Am. Chem. Soc.* **2006**, *128*, 16655–16663.

(27) Chen, X.; Bu, Y. *J. Am. Chem. Soc.* **2007**, *129*, 9713–9720.

(28) Tishchenko, O.; Truhlar, D. G.; Ceulemans, A.; Nguyen, M. T. *J. Am. Chem. Soc.* **2008**, *130*, 7000–7010.

(29) Hatcher, E.; Soudackov, A. V.; Hammes-Schiffer, S. *J. Am. Chem. Soc.* **2004**, *126*, 5763–5775.

(30) Pratt, R. C.; Stack, T. D. P. *J. Am. Chem. Soc.* **2003**, *125*, 8716–8717.

(31) (a) Carra, C.; Iordanova, N.; Hammes-Schiffer, S. *J. Am. Chem. Soc.* **2003**, *125*, 10429–10436. (b) Sjodin, M.; Styring, S.; Wolpher, H.; Xu, Y.; Sun, L.; Hammarstrom, L. *J. Am. Chem. Soc.* **2005**, *127*, 3855–3863. (c) Sjodin, M.; Irebo, T.; Utas, J. E.; Lind, J.; Merenyi, G.; Akermark, B.; Hammarstrom, L. *J. Am. Chem. Soc.* **2006**, *128*, 13076–13083. (d) Concepcion, J. J.; Brennaman, M. K.; Deyton, J. R.; Lebedeva, N. V.; Forbes, M. D. E.; Papanikolas, J. M.; Meyer, T. J. *J. Am. Chem. Soc.* **2007**, *129*, 6968–6969. (E) Kumar, M.; Kozlowski, P. M. *J. Phys. Chem. B* **2009**, *113*, 9050–9054.

(32) Meunier, B.; de Visser, S. P.; Shaik, S. *Chem. Rev.* **2004**, *104*, 3947–3980.

(33) (a) Nocek, J. M.; Zhou, J. S.; De Forest, S.; Priyadarshy, S.; Beratan, D. N.; Onuchic, J. N.; Hoffman, B. M. *Chem. Rev.* **1996**, *96*, 2459–2490. (b) Tanaka, M.; Ishimori, K.; Mukai, M.; Kitagawa, T.; Morishima, I. *Biochemistry* **1997**, *36*, 9889–9898.

(34) (a) Barry, B.; Babcock, G. T. *Proc. Natl. Acad. Sci. U.S.A.* **1987**, *84*, 7099–7103. (b) Tommos, C.; Babcock, G. T. *Acc. Chem. Res.* **1998**, *31*, 18–25. (c) Loll, B.; Kern, J.; Saenger, W.; Zouni, A.; Biesiadka, J. *Nature* **2005**, *438*, 1040–1044.

(35) (a) Volbeda, A.; Fontecilla-Camps, J. C. *Coord. Chem. Rev.* **2005**, *249*, 1609–1619. (b) Peters, J. W.; Lanzilotta, W. N.; Lemon, B. J.; Seefeldt, L. C. *Science* **1998**, *282*, 1853–1858.

(36) Frisch, M. J.; *Gaussian 03*, revision C.02; Gaussian, Inc.: Wallingford, CT, 2004.

(37) (a) Becke, A. D. *J. Chem. Phys.* **1993**, *98*, 5648–5652. (b) Lee, C.; Yang, W.; Parr, R. G. *Phys. Rev. B* **1988**, *37*, 785–789.

(38) (a) Ditchfield, R.; Hehre, W. J.; Pople, J. A. *J. Chem. Phys.* **1971**, *54*, 724–728. (b) Hehre, W. J.; Ditchfield, R.; Pople, J. A. *J. Chem. Phys.* **1972**, *56*, 2257–2261. (c) Hariharan, P. C.; Pople, J. A. *Theor. Chim. Acta* **1973**, *28*, 213–222. (d) Hariharan, P. C.; Pople, J. A. *Mol. Phys.* **1974**, *27*, 209–214. (e) Gordon, M. S. *Chem. Phys. Lett.* **1980**, *76*, 163–168. (f) Francl, M. M.; Pietro, W. J.; Hehre, W. J.; Binkley, J. S.; Gordon, M. S.; Defrees, D. J.; Pople, J. A. *J. Chem. Phys.* **1982**, *77*, 3654–3665.

(39) Kendall, R. A.; Dunning, T. H.; Harrison, R. J. *J. Chem. Phys.* **1992**, *96*, 6796–6806.

(40) (a) Gonzalez, C.; Schlegel, H. B. *J. Phys. Chem.* **1990**, *94*, 5523–5527. (b) Ishida, K.; Morokuma, K.; Kormornicki, A. *J. Chem. Phys.* **1977**, *66*, 2153–2156. (c) Gonzalez, C.; Schlegel, H. B. *J. Chem. Phys.* **1989**, *90*, 2154–2161.

(41) Delley, B. *J. Chem. Phys.* **1990**, *92*, 508–517.

(42) *Cerius2*; BIOSYM/Molecular Simulations: San Diego, CA, 1996.

(43) Beche, A. D. *J. Chem. Phys.* **1988**, *88*, 2547–2553.

(44) (a) Liu, Y.; Tuckerman, M. E. *J. Chem. Phys.* **2000**, *112*, 1685–1700. (b) Windiks, R.; Delley, B. *J. Chem. Phys.* **2003**, *119*, 2481–2487.

(45) (a) Adir, N.; Lerner, N. *J. Biol. Chem.* **2003**, *278*, 25926–25932. (b) Schmidt, M.; Krasselt, A.; Reuter, W. *Biochim. Biophys. Acta* **2006**, *1764*, 55–62. (c) Schmidt, M.; Patel, A.; Zhao, Y.; Reuter, W. *Biochemistry* **2007**, *46*, 416–423. (d) Stec, B.; Troxler, R. F.; Teeter, M. M. *Biophys. J.* **1999**, *76*, 2912–2921.

(46) Chen, X.; Xing, D.; Zhang, L.; Cukier, R. I.; Bu, Y. *J. Comput. Chem.* **2009**, *30*, 2694–2705.

(47) Galian, R. E.; Pastor-Pérez, L.; Miranda, M. A.; Pérez-Prieto, J. *Chem.—Eur. J.* **2005**, *11*, 3443–3448.

(48) (a) Morozova, O. B.; Yurkovskaya, A. V.; Vieth, H.-M.; Sagdeev, R. Z. *J. Phys. Chem. B* **2003**, *107*, 1088–1096. (b) Morozova, O. B.; Yurkovskaya, A. V.; Sagdeev, R. Z. *J. Phys. Chem. B* **2005**, *109*, 3668–3675.

(49) Chen, X.; Zhang, L.; Wang, Z.; Li, J.; Wang, W.; Bu, Y. *J. Phys. Chem. B* **2008**, *112*, 14302–14311.

(50) It is necessary to point out that the structure of the product ($TrpGly_nTyr^{\bullet}\cdots AH$) obtained by DFT optimizations is not completely the same as that in the dynamics simulation processes. This is because that DFT optimizations give minima on the potential energy surface, and AIMD simulations give transient conformational states to favor proton/electron transfer.

(51) Seyedsayamdost, M. R.; Yee, C. S.; Reece, S. Y.; Nocera, D. G.; Stubbe, J. *J. Am. Chem. Soc.* **2006**, *128*, 1562–1568.

JP9077689